Selective catalytic oxidation of alkylaromatic molecules by nanosize water droplets containing Co^{2+} species in supercritical carbon dioxide fluid

Shik Chi Tsang[a]; Jie Zhu[a]; Kai Man K. Yu[a]

[a] Department of Chemistry, Surface and Catalysis Research Centre, Whiteknights, Reading RG6 6AD, UK

PLEASE SCROLL DOWN FOR ARTICLE

Selective catalytic oxidation of alkylaromatic molecules by nanosize water droplets containing Co^{2+} species in supercritical carbon dioxide fluid

SHIK CHI TSANG*, JIE ZHU and KAI MAN K. YU

Department of Chemistry, Surface and Catalysis Research Centre, University of Reading, Whiteknights, Reading RG6 6AD, UK

Stabilized *nano-sized* water droplet carrying water-soluble Co^{2+} species is employed as a new catalyst system for the oxidation of the alkyl aromatics in the presence of a fluorinated surfactant. This stable system contains no labile C–H structure and can facilitate excellent mixing of catalytic Co(II)/NaBr species, hydrocarbon substrates and oxygen in supercritical carbon dioxide fluid, which is demonstrated to be an excellent alternative solvent system to acetic acid or nitric acid for air oxidation of a number of alkyl aromatic hydrocarbons using Co(II) species at mild conditions. As a result, potential advantages of this 'greener' catalytic method including safer operation, easier separation and purification, higher catalytic activity with selectivity and without using corrosive or oxidation unstable solvent are therefore envisaged.

Keywords: Supercritical carbon dioxide; Oxidation; Microemulsion; Nanosize; Water droplet; Alkyl aromatic hydrocarbons; Catalysis; Selectivity

1. Introduction

Partial oxidation of hydrocarbons with air or molecular oxygen is a commercially important process for production of oxygenated compounds in the chemical industry [1]. Small partially oxygenated hydrocarbons are widely used as building blocks in the manufacture of plastics and synthetic fibres. Many oxygenates also play important roles as intermediates in the syntheses of fine chemicals. Table 1 summarises several commercially important processes concerning oxidation of alkyl aromatic hydrocarbons [1]. As seen from the table the production volumes of the chemicals listed are impressive and serve to underline their importance in industry. In terms of tonnages,

Table 1.　Major chemical processes utilizing alkyl aromatic hydrocarbon oxidation [1].

Product	Capacity 10^6 tpy*;	Oxidation step	Important processes	Main application
Terephthalic acid (PTA)	11.38 (1995[#])	*p*-Xylene to terephthalic acid	Amoco Mid-Century	PET (fiber, film, resin)
Dimethyl terephthalate (DMT)	4.06 (1995[#])	*p*-Xylene to terephthalic acid to DMT	Witten, BASF, Dupont	PET (fiber, film, resin)
Cumyl hydroperoxide	6.5 (1998[#])	Cumene to cumyl hydroperoxide	Hock (BP, Kellogg)	Phenol
Benzoic acid	0.28 (1995[#])	Toluene to benzoic acid	DSM, Dow	Phenol, salt, ester of benzoic acid

*tpy = Tons per year; [#]The year when the capacity was produced.

the conversion of *p*-xylene to PTA and dimethyl terephthalate (DMT) ranked as the highest among the oxidation processes.
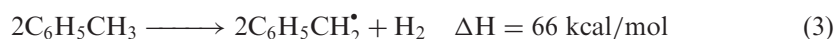
The first recorded process for the production of terephthalic acid from *p*-xylene used nitric acid as an oxidant. This process took place in the liquid phase at a temperature between 150°C and 200°C and at a pressure between 8 bar to 13 bar (total pressure) in dilute nitric acid (30–40 wt.%) [2, 3]. The disadvantages of this oxidation process included a large amount of lower oxides of nitrogen being generated (decomposition of nitric acid), a high risk of an explosion hazard and the difficulties for product purification. The second recorded oxidation process was so called 'Mid-Century' process, which is still currently the most popular process for the partial oxidation of *p*-xylene. The process involves the use of bromide-promoted heavy metal catalysts such as cobalt and manganese ions in acetic acid solution under 175–230°C and 23–26 bar [4, 5]. The results of the oxygenation of 251 hydrocarbons using this method have been reviewed [6] accounting this process as one of the current major industrial processes for producing oxygenates from hydrocarbon oxidations (equation (1)):

$$\text{Hydrocarbon} + O_2 \xrightarrow[\text{Acetic acid}]{\text{Metal/bromide}} \text{Oxygenate} + H_2O \qquad (1)$$

As seen from the table 1, partial oxidation of toluene is also an important process in industry. 0.28 million tons of benzoic acid was produced in 1995 mainly by the two processes (Dow and Snia Viscosa). In these processes, the reactions were usually performed with a cobalt catalyst and a promoter in acetic acid solution at a temperature between 110–165°C and a pressure between 2–9 bar [7]. The partial oxidation of toluene is among the most extensively investigated systems because it has been chosen as a model reaction for the study of oxidation kinetics and methods of predicting optimum reactor design and operational conditions [8].

Concerning the mechanisms of toluene oxidation, it is well known that dioxygen, with its triplet ground spin state, does not react easily with hydrocarbons (i.e. toluene) at mild conditions since they exist in a singlet ground state. One could therefore initiate an auto-oxidation if a hydrocarbon radical is produced by breaking a C–H bond since the radical would then react rapidly with triplet dioxygen at room temperature [9].

However, the radicals of hydrocarbons are not easily prepared as the strength of C–H bond is in the range of 70–100 kcal/mol, such as equations (2) and (3):

$$C_6H_5CH_3 \longrightarrow C_6H_5CH_2^{\bullet} + H^{\bullet} \quad \Delta H = 85 \text{ kcal/mol} \tag{2}$$

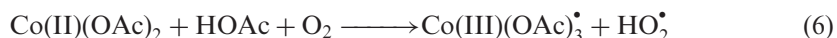$$2C_6H_5CH_3 \longrightarrow 2C_6H_5CH_2^{\bullet} + H_2 \quad \Delta H = 66 \text{ kcal/mol} \tag{3}$$

Thus the high bond dissociation energy of C–H in hydrocarbons prevents the formation of radical below 500°C [10]. It is possible to produce hydrocarbon radicals thermally by reacting the hydrocarbon directly with dioxygen at elevated temperatures. However, the initial one-electron reduction potential is only −0.2 V. The heat produced from the reaction of dioxygen with hydrocarbons to form radicals has been estimated to be strongly endothermic and the formation of radicals is therefore negligible below 300°C [11], such as equations (4) and (5):

$$RCH_3 + O_2 \longrightarrow RCH_2^{\bullet} + HO_2^{\bullet} \quad \Delta H = 38 \text{ kcal/mol} \tag{4}$$

$$2RCH_3 + O_2 \longrightarrow 2RCH_2^{\bullet} + H_2O_2 \quad \Delta H = 41 \text{ kcal/mol} \tag{5}$$
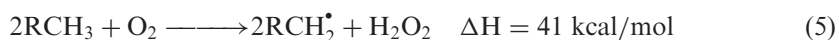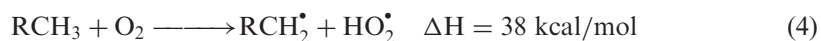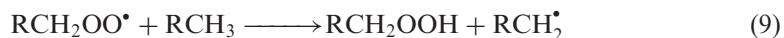
The high temperature oxidation processes could lead to uncontrolled subsequent oxidations of the molecules leading to undesirable degraded products. As a result, transition metal ion species as catalysts such as Co^{2+} are commonly used in the Mid-Century oxidation processes at mild conditions. Thus, the conservation of spin rule can be avoided by having dioxygen initially interact with cobalt species, which allows the initiation of classical radical chain reactions during the oxidation process as follows [12].
Initiation:

$$Co(II)(OAc)_2 + HOAc + O_2 \longrightarrow Co(III)(OAc)_3^{\bullet} + HO_2^{\bullet} \tag{6}$$

$$Co(III)(OAc)_3^{\bullet} + RCH_3 \longrightarrow Co(II)(OAc)_2 + RCH_2^{\bullet} + HOAc \tag{7}$$

Propagation:

$$RCH_2^{\bullet} + O_2 \longrightarrow RCH_2OO^{\bullet} \tag{8}$$

$$RCH_2OO^{\bullet} + RCH_3 \longrightarrow RCH_2OOH + RCH_2^{\bullet} \tag{9}$$

Chain Branching:

$$RCH_2OOH + Co(II)(OAc)_2 + HOAc \longrightarrow RCH_2O^{\bullet} + H_2O + Co(III)(OAc)_3 \tag{10}$$

$$RCH_2O^{\bullet} + RCH_3 \longrightarrow RCH_2OH + RCH_2^{\bullet} \tag{11}$$
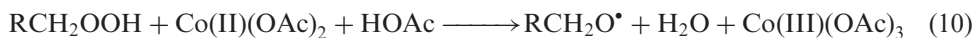
According to the general accepted scheme 1 [6], Co(II) will be oxidised to Co(III) in the presence of oxygen or peroxide species. Co(III) acetate in acidic water, having a redox
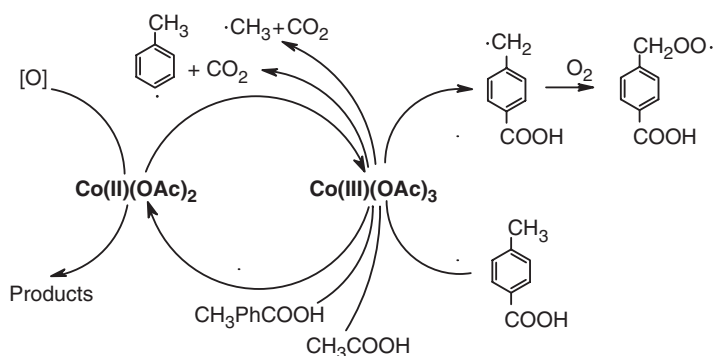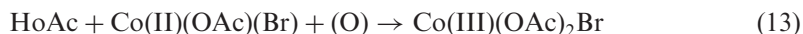
potential of 1.9 V, is one of the strongest oxidants known in chemistry. Thus, the
Co(III) can then initiate (or propagate) the chain reactions by reacting with the methyl
aromatic molecule. It is well established that cobalt (III) exists in a number of different
forms in acetic acid, these involve monomers and polymers of cobalt (III) and mixed-
valence Co(II)/Co(III) complexes. Included in this figure are two important side
reactions: the decarboxylation of acetic acid (solvent) and *p*-toluic acid (or any other
aromatic acid present) by Co(III). It is interesting to note that the rate of desired
reaction cannot be enhanced by simply increasing temperature since the side reactions
become more and more pronounced at higher temperatures and these acids compete for
the Co(III) moiety with *p*-toluic acid. The cobalt(III) assisted acetic acid oxidation
(oxidation of solvent) becomes more favourable than the cobalt(III)-methylbenzene
oxidation (oxidation of substrate) at temperatures higher than 130°C [6].

One can enhance the rate of oxidation by adding a reagent that oxidizes the Co(II)
to Co(III), which keeps a steady high concentration of Co(III) and thus pushes the
reaction to completion. In this way, acetaldehyde, paraldehyde, and 2-butanone have
been used to co-oxidize the cobalt [13, 14].

Bromide is a well-known promoter in this system. It has been suggested that most
of the bromide added is coordinated to the cobalt(II) as the equation (12) gives a
equilibrium constant (K) of 800 [15]:

$$Co(II)(OAc)_2 + HBr \rightleftharpoons Co(II)(OAc)(Br) + HOAc \quad K = 800 \qquad (12)$$

The oxidation of the cobalt(II) bromide complex will produce a transitory Co(III)
complex, which rapidly undergoes an intra-molecular electron transfer to a Co(II)
bromide complex by dissociating or reacting directly with the methylbenzene to produce
the radical (equations (13) and (14)):

$$HoAc + Co(II)(OAc)(Br) + (O) \rightarrow Co(III)(OAc)_2Br \qquad (13)$$

$$Co(III)(OAc)_2Br + C_6H_5CH_3 \rightarrow Co(II)(OAc)_2 + HBr + C_6H_5CH_2^{\bullet} \qquad (14)$$

Scheme 1. Catalytic cycles in which the generated peroxides propagate the formation of the radical of
p-toluic acid.

It is believed that the Co(III) bromide complexes have greater activity than the original Co(III) and it is highly possible that the bromide radical becomes a chain carrier. Both of these effects increase the rate of reaction (a factor as high as 300 has been reported [16]). In the presence of bromide, the steady-state Co(III) concentration decreases because of the rapid intramolecular electron transfer to bromide, this slows down decarboxylation and thus improves the product selectivity.

Despite the great successes of these traditional oxidation processes for the oxidation of a wide range of alkyl aromatic hydrocarbons in liquid phase, problems resulted from the decarboxylation of the organic solvent (acetic acid) due to the unselective oxidation, downstream treatments associated with the use of extremely corrosive and toxic acetic acid, difficulties in solvent and catalyst recovery, and explosion hazards associated with solvent and dioxygen at high concentration (with reported explosions) are clearly evident [17]. With increasingly demanding environmental legislation and public and corporate pressure, a new process is urgently required to replace the current processes [18]. Many attempts have been made at developing solid catalysts containing transition metal ions [19–22]. Two approaches were generally utilised. One was liquid-phase oxidation, in which the reactions were carried out either in liquid substrate without any solvent, or in less toxic organic solvents. In these processes, the explosion hazards associated with solvent and dioxygen at high concentration remains a big hurdle. Moreover, the catalyst stability and metal leaching presently exclude them from existing applications [23]. The other approach was gas phase oxidation, in which Mo-based and V-based oxides supported on TiO_2 modified by SeO_2, TeO_2 or Sb_2O_3 were identified to be the best catalysts for selective oxidation of toluene to gain high conversion and considerable selectivity [24]. Unfortunately, the catalysts were poorly active at mild temperatures and had to be operated at a relatively high temperature (most of them are run above $350°C$) in the gas phase. Thus these approaches resulted in a poor carbon balance because of total oxidation of the substrate. In fact, at least 20% of the starting hydrocarbon is being still converted to CO_x ($CO + CO_2$) at high conversions according to the recent papers [24–27]. Therefore, much attention had to be focused on the treatment of the reaction temperature since hot spots might be easily generated in the gas phase due to the exothermic reaction ($C_6H_5CH_3 + 3/2 O_2 = C_6H_5COOH + H_2O$, $\Delta H = -134\,kcal/mol$).

Supercritical carbon dioxide fluid ($scCO_2$) has recently received considerable attention as a new versatile, environmentally friendly medium for a variety of catalytic reactions, these include free-radical polymerisation [28], hydroformylation [29], hydrogenation [30], and partial oxidations [31]. Its non-toxic, non-combustible and non-flammable nature combined with the ease of solvation of some organic substrates in the inexpensive medium and ease of pressure facilitated separation may offer an exciting possibility of replacing acetic acid for catalytic partial oxidations. $scCO_2$ is, in particular, suitable for the oxidation of alkyl aromatic hydrocarbons since: (i) it can dissolve hydrocarbons with good solubilities because of their low polarities; (ii) the catalyst deactivation (chain termination) due to solvent decarboxylation in traditional processes can be avoided since CO_2 can not be further oxidized; (iii) the by-products generated from solvent decarboxylation can be eliminated. Despite these encouraging facts, a major limitation for the use of $scCO_2$ as a reaction medium is its inability to dissolve hydrophiles, in particular the ionic catalyst/promoter species that are required

for the oxidation ($Co^{2+}/NaBr$). Recent work has shown that a number of fluorinated surfactants were able to form aqueous micro-emulsion in $scCO_2$ [32, 33]. Similarly, other fluorinated species are also able to modify the interfacial tension of the water-CO_2 interface forming a metastable aqueous emulsion [34]. Thus, fluorinated surfactants and related compounds are able to disperse water-soluble metal salt in the non-polar $scCO_2$ medium. Moreover, these fluorinated surfactants are far more stable than their hydrocarbons analogues since the dissociation energy of a typical C-F bond (i.e. 124 kcal/mol for CF_3-F) is much higher than that of a C–H bond (i.e. 104 kcal/mol for CH_3-H) [25]. It is well accepted that the existence of C–H bonds in a solvent or a catalyst system during the oxidation of hydrocarbon should be avoided because they have the possibility to be oxidised. Hence, the water-CO_2 micro-emulsion containing cobalt species in the presence of a fluorinated surfactant may be an ideal nano-catalyst system for the oxidation of hydrocarbons in $scCO_2$ because no C–H bond exists in either the catalyst system or the solvent.

The authors were therefore particularly keen to employ aqueous micro-emulsion droplets as *nano-reactor* carrying catalytically active species in supercritical carbon dioxide fluid for catalytic oxidation. As a result, it is reported in an earlier communication note that anionic fluorinated surfactant ions chelated with Co(II) denoted as F-Co(II) can serve as surfactant and catalyst for the oxidation of toluene [31]. In this paper, further detailed and comprehensive studies on the effects of water content, NaBr concentration, substrate concentration, oxygen concentration, pressure and temperature on the activity of this nano-catalyst system are presented.

2. Experimental

2.1 *Synthesis of F-Co(II)*

2.0 mmol nonadecafluorodecanoic acid ($CF_3(CF_2)_8COOH$, designated as NDFDA, 98%; Aldrich) was dissolved in 25 mL pre-dried diethyl ether. Thereafter, the fresh cobalt carbonate (synthesized in the previous step) was added into the mixture. It was observed that small bubbles (CO_2) were generated on the surface of the solid. The mixture was refluxed at 40°C (oil bath temperature) for 12 hours. It was found that the colour of the solution became red since the generated $[CF_3(CF_2)_8COO]_2Co(II)$ (designated as F-Co(II)) is highly soluble in diethyl ether. The residue (excess of $CoCO_3$) was removed by filtration with exhaustive washing using diethyl ether. The resulting solution from the filtration was air dried at room temperature and a pink solid was collected. This solid was then re-dissolved in small amount of diethyl ether. Purification of this F-Co(II) was achieved by allowing the solution to pass through a silica gel (0.035–0.070 mm diameter in size, pore diameter ca 6 nm, Aldrich) packed column (ca 0.7 cm inner diameter and 28 cm length) with diethyl ether as the mobile phase. The pink layer (the second layer) was collected. A pink solid was obtained once the solvent was evaporated at room temperature, which accounted a yield of 76.1% depended on NDFDA.

$$CoCO_3 + 2CF_3(CF_2)_8COOH \longrightarrow [CF_3(CF_2)_8COO]_2Co + H_2O + CO_2 \qquad (15)$$
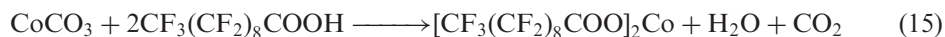
2.2 *Characterization of F-Co(II)*

The infrared spectra presented in figure 1 shows a strong C=O stretch absorption at $1653\,cm^{-1}$ (strong and sharp) in the carboxylic anion form for F-Co(II) while the NDFDA has only a relatively weaker absorption at $1717\,cm^{-1}$ (weak and broad) in the acid form. This shift of the C=O stretch absorption was attributed to the delocalization of the electron density of carbonyl group by the Co^{2+}. This phenomenon was also observed in the standard IR spectra of stearic acid and its sodium salt [35, 36]. This shift can be utilized to monitor the purity of the F-Co(II).

The UV-vis spectrum of F-Co(II) (diethyl ether as solvent) presented in figure 2 shows two maxima, λ_1 at 208 nm, $\varepsilon_1 = 5.35 \times 10^4\,dm^3mol^{-1}cm^{-1}$; λ_2 at 520 nm, $\varepsilon_2 = 1430\,dm^3mol^{-1}cm^{-1}$. The second peak is attributed to the Co^{2+} that can be used to differentiate F-Co(II) from its acid form (NDFDA). Microanalysis and atomic absorption indicated that the material is composed of $(CF_3(CF_2)_8CO)_{1.95}Co \cdot 4H_2O$. The melting point of this material was also determined. It was found to be in the range of 138–140°C, which is different from that of NDFDA (83–85°C).

2.3 *Measuring the solubility of toluene in scCO₂*

In this work, toluene was selected as a model substrate for investigating the catalytic activities of catalyst systems. Hence the solubility of toluene was measured under the reaction conditions (under which the catalytic tests were carried out) with a small amount of benzene (20 μL) as an internal standard using a Gas Chromatograph (GC).
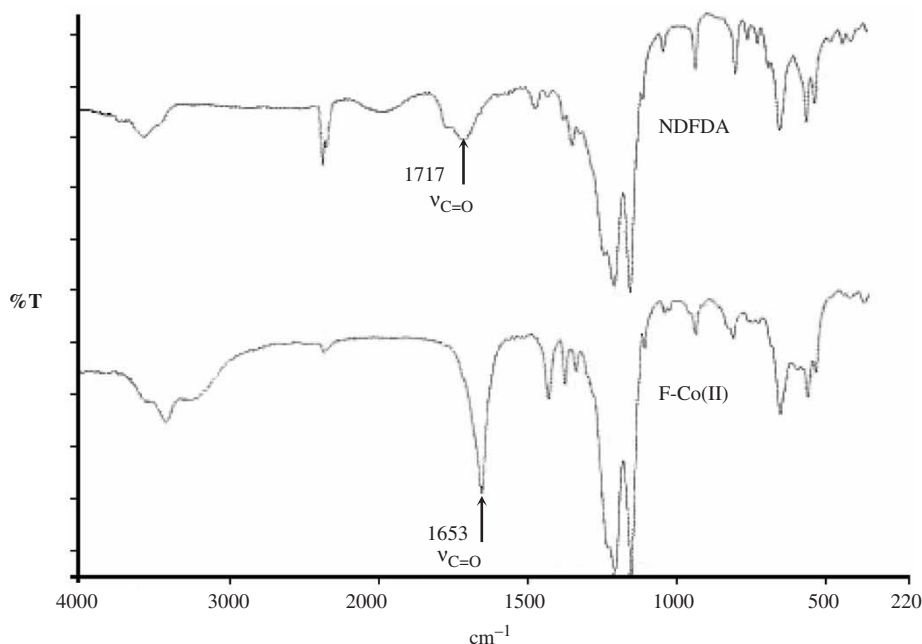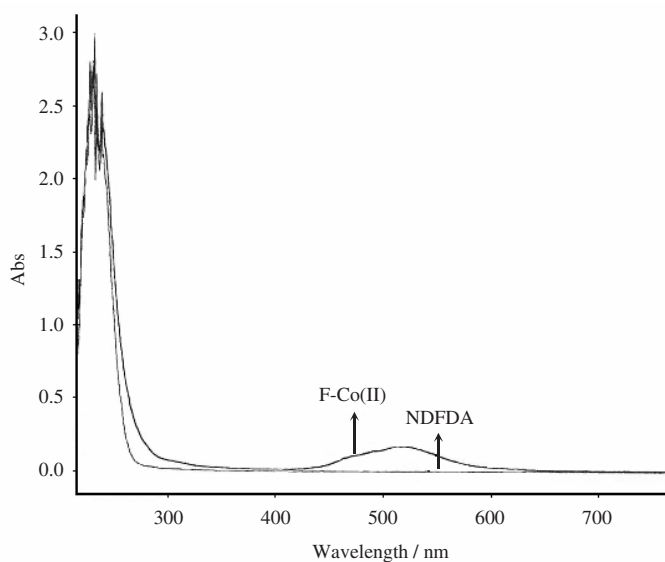

Figure 1. FTIR spectra of F-Co(II) and NDFDA.

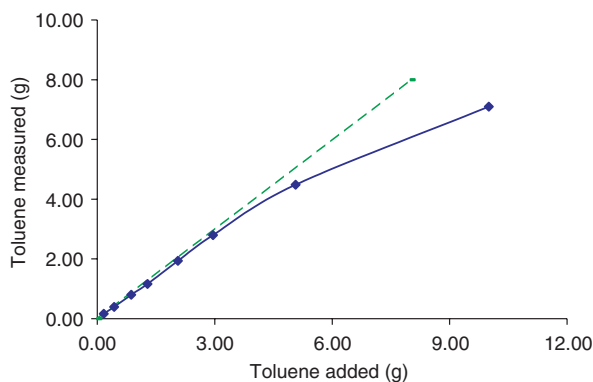Figure 2.   UV-visible spectra of F-Co(II) and ADFDA.

Figure 3.   The solubility of toluene in scCO$_2$.

The amount of benzene used was completely soluble in scCO$_2$ under the experimental conditions [37]. In this strategy, only the dissolved toluene in scCO$_2$ was detected. If the toluene is completely soluble in scCO$_2$, the detected ratio of toluene/benzene should be equal to the ratio initially added. In each case, the analysis was carried out after stirring for 2 hours at 120°C under 150 bar. It can be seen from figure 3 that at least 3.0 g (32.6 mmol) of toluene could be dissolved in 111 mL scCO$_2$ under our experimental conditions.

2.4 *Catalytic activity test*

All the catalytic activity experiments were thus carried out in a 160 mL Parr autoclave with a Teflon cup insert, this cup protected against corrosion in the batch process.

The valid volume of the reactor was 111 mL. The surfactant, catalysts and substrate were added into the autoclave directly, this was followed by the addition of a trace amount of internal standard (20 μL benzene). Thereafter, 10 bar dioxygen (BOC Gases) was directly charged into the autoclave from cylinder and then carbon dioxide (BOC Gases) was pumped into the autoclave using a booster to a desired pressure. The mixture was then stirred at the set temperature for the desired reaction time. The stirrer motor was set at ½ maximum speed, giving approximately 360 rpm. Toluene content was online monitored using a GC. At the end of the reaction, high boiling products were collected. The obtained solution (containing reaction mixture) were analysed quantitatively using a HPLC instrument.

3. Results and discussions

### 3.1 *Oxidation of toluene using nano-water droplet containing Co(II)*

3.1.1 The activity of F-Co(II). Table 2 shows the results of partial oxidation of toluene using O_2 in $scCO_2$ after a 12 hour reaction time. It was found that the dehydrated F-Co(II) was not significantly effective as a catalyst in the absence of water (entry 1). However, with the addition of a small amount of water (100 μL), it was interesting to find that F-Co(II) was extremely active (>95% conversion) and selective (>99% to benzoic acid) for the oxidation of toluene in $scCO_2$ in the presence of either NaBr (entry 2) or HBr (entry 3). But it was poorly active under the same experimental conditions without bromide addition (entry 4). From these results, the presence of water (entry 1 vs. entry 2) and the ionic bromide promoter (entries 2, 3 vs. entry 4) appeared to be important for an optimum catalytic system.

Modification of organometallic complexes with fluorinated tails to render a complex soluble in $scCO_2$ has been well documented [38, 39]. However, the possibility of the F-Co(II) acting as a homogeneous catalyst in $scCO_2$ could be discounted. This is because the dehydrated F-Co(II) *in the absence of water* is not effective in catalysing the oxidation. Also, the role of NaBr as a promoter cannot be elucidated by homogeneous catalysis because NaBr is absolutely insoluble in $scCO_2$. On the other hand, it is well documented that many fluorinated surfactants similar to the F-Co(II) discussed can form micro-emulsion in $scCO_2$ [32, 33, 40]. This strongly suggests that the formation of micro-emulsion in $scCO_2$ might be involved in this system. The authors envisage that

Table 2. The oxidation of toluene (18.8 mmol) oxidation in the presence of 0.1 mL H_2O in 150 bar (total pressure) CO_2.

Entry	Catalyst	Promoter	T/°C	Conv. (%)	Benzoic acid (% select.)
1	0.25mmol dehydrated F-Co(II)*	0.2 mmol NaBr	140	14.2	91.2
2	0.25mmol F-Co(II)	0.2 mmol NaBr	120	98.2	99.1
3	0.25mmol F-Co(II)	0.2 mmol HBr (48%)	120	95.5	99.9
4	0.25mmol F-Co(II)	Nil	140	6.0	68.8

*No water was added.
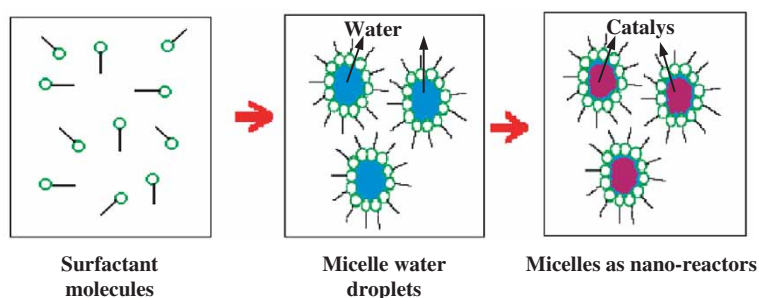
Scheme 2.   Catalysis taken place in reverse micelles in $scCO_2$ as nanoreactors.

F-Co(II) might act as fluorinated surfactant to form micro-emulsion in a water-CO_2 mixture with its counterion (Co^{2+}) working as the catalyst. The promoter (sodium bromide) can be dissolved in the core of this reverse micelle (scheme 2). If this assumption is true, it provides a means of bringing species of very different polarities into contact with each other with excellent mass and heat transfers whilst sustaining a fast catalytic reaction. It is noted that $scCO_2$ fluid is also proved to be the essential medium to form the micro-emulsion with the mixture since if $scCO_2$ was replaced by same pressure of N_2, low activity (3.9% conversion) was observed under the identical conditions.

3.1.2 The effect of water on catalysis.   Since water is essential in establishing the nano-catalytic system. Hence, carefully controlled experiments were designed to monitor toluene conversions over catalysts (0.25 mmol F-Co(II), 0.2 mmol NaBr) with varying water contents (100, 200, 300 and 500 µL water, respectively) at 120°C. The results presented in figure 4 suggest that the general conversion versus time curves comprise an exponential phase (reaching steady activity) with an initial induction period (much slower rate), **I**, for all catalysts. Presumably, the induction period involves the buildup of the concentrations of radicals (and/or other active species) to the critical level needed to ignite the reaction. It is noted that activity (expressed as *turnover frequency* in the rate-stable region after induction period, designated as TOF) and length of induction (**I**) depend critically on water content. It is well known that $scCO_2$ can dissolve water in its phase. Some of the water is needed to pre-saturate the $scCO_2$ phase before it can appear as micro-emulsion droplets. Thus, these results suggest that micro-emulsion may not be formed particularly if insufficient amounts of water are initially used during the induction period at low W values (molar water to F-Co(II) ratios). However, oxidation of toluene will yield additional quantities of water (by-product) to assist micelles formation (18.8 mmol for 100% conv.). Hence this can account for the abrupt increase in activity after the induction period (in the case of $W = 22$). Based on the activity curves, it can be estimated that a minimum of about 270–310 µl water is required before the establishment of the micro-emulsion. Despite the actual water solubility depending on conditions and impurities (substrates and products) in $scCO_2$ this value is in a general agreement with Wiebe's calculations [41].

It is noted that the measured activity over this nano-reactor system in $scCO_2$ at 120°C ($6.48 \times 10^{-3} \, s^{-1}$) was extremely promising for toluene oxidation which was more than
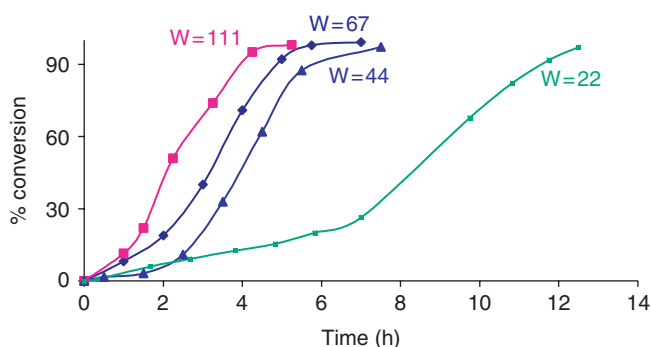
Figure 4. Monitoring of toluene conversions using various H_2O quantities (TOF $= 3.14 \times 10^{-3}\,s^{-1}$, I $= 7\,h$ at W $= 22$; TOF $= 6.07 \times 10^{-3}\,s^{-1}$, I $= 2.5\,h$ at W $= 44$; TOF $= 6.48 \times 10^{-3}\,s^{-1}$, I $= 1.5\,h$ at W $= 67$; TOF $= 6.19 \times 10^{-3}\,s^{-1}$, I $= 1.0\,h$ at W $= 111$) under the typical conditions: 0.25 mmol F-Co(II); 0.2 mmol NaBr; 18.8 mmol toluene; 20 μL benzene used as internal standard; 10 bar O_2 and 150 bar CO_2 at 120°C.

27 times higher than the reported rate of $2.4 \times 10^{-4}\,s^{-1}$ (87°C) in Co^{2+}/water/acetic acid [42] and 100 times higher than the solid counterpart in $scCO_2$ ($1 \times 10^{-5}\,s^{-1}$ at 140–200°C [43]). Although the values of rate difference should not be taken too literally without comparing activity under identical conditions, the excellent activity of the aqueous micro-emulsion catalyst in water-$scCO_2$ is apparent. Such high activity is attributed to the intrinsically faster mass transfers in water-$scCO_2$ than in liquid and the dynamic properties of the small micro-emulsion droplets.

3.1.3 Visual inspection through sapphire windows. Experiments were designed to shed light on the catalytic working state using a Parr reactor equipped with sapphire windows. Under the experimental conditions (0.25 mmol F-Co(II), 0.2 mmol NaBr), it was revealed that most of the F-Co(II) was insoluble in $scCO_2$ *in the absence of water* under the temperatures ranging from 25°C to 120°C. Thus the interactions of the fluorinated tail of F-Co(II) with $scCO_2$ are apparently unable to override the stronger ionic interactions within solid in the absence of water. On the other hand, with the addition of 400 μL water, it was observed that although the F-Co(II) was insoluble in liquid CO_2 at 25°C (figure 5a), by increasing the operating temperature, the boundary of liquid CO_2 became more and more obscure and the mixture became misty at the same time. Thereafter, the boundary completely disappeared and then the mixture became opaque at approximately 35°C. Interestingly, the opaque mixture became a transparent fluid with no phase boundary under stirring at elevated temperature (~80°C) in $scCO_2$ (figure 5b). It is worth noting that the formation of micro-emulsion in $scCO_2$ giving a characteristic transparent fluid has also been reported [32]. When the reactor was cooled down, a misty stage was observed again before CO_2 liquefaction.

Separate experiments performed under atmospheric conditions have shown that F-Co(II) is insoluble in water but immediately forms cloudy colloids when stirred at room temperature. These results suggested that F-Co(II) functions like a surfactant rather than a homogeneous catalyst.
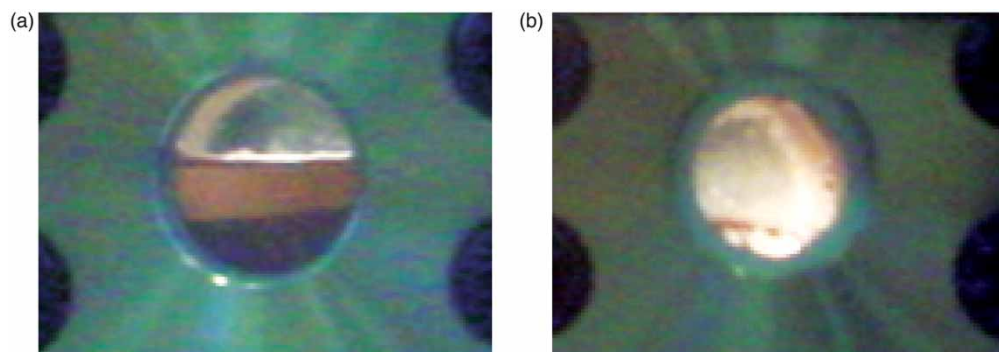
Figure 5. Visual inspection through reactor equipped with sapphire windows (a) a catalyst slurry at 25°C, ~67 bar (with liquid CO_2); (b) reaching a transparent state at 120°C, ~150 bar CO_2.

Figure 6. F-Co(II)/NaBr before (L) and after reaction (R).

3.1.4 Postmortem analysis of nano-catalyst system. To further reveal the catalysis working state a detailed postmortem analysis was carried out after a rapid de-pressurisation of the system (0.25 mmol F-Co(II)/20 mg NaBr/400 μL H_2O) from the typical conditions (120°C and 150 bar). This gave a solid foam (figure 6 right). The volume of the solid foam was much larger than the powder initially added (figure 6 left). The colour of the powder was also observed to become less pink. These may indicate some subtle changes in either the physical properties (i.e. becoming smaller particles) or the chemical properties (forming new complex) of the catalyst mixture.

The resulting solid foam was analysed by TEM. The TEM micrograph (figure 7a) of the solid foam indicates uniform size NaBr crystallites of approximately 3 ± 2 nm extremely well-dispersed in non-crystalline F-Co(II) matrices. EDAX mapping (figure 8) of the material using a nano-probe (27.5 nm diameter) gives a constant atomic Br/Co ratio of 0.16 ± 0.03 (calibrated against $CoBr_2$) indicative of
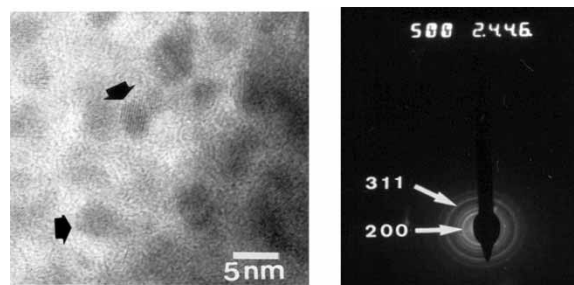
Figure 7. a (left) The TEM micrograph of the solid after reaction; b (right) An electron diffraction pattern of the solid foam.
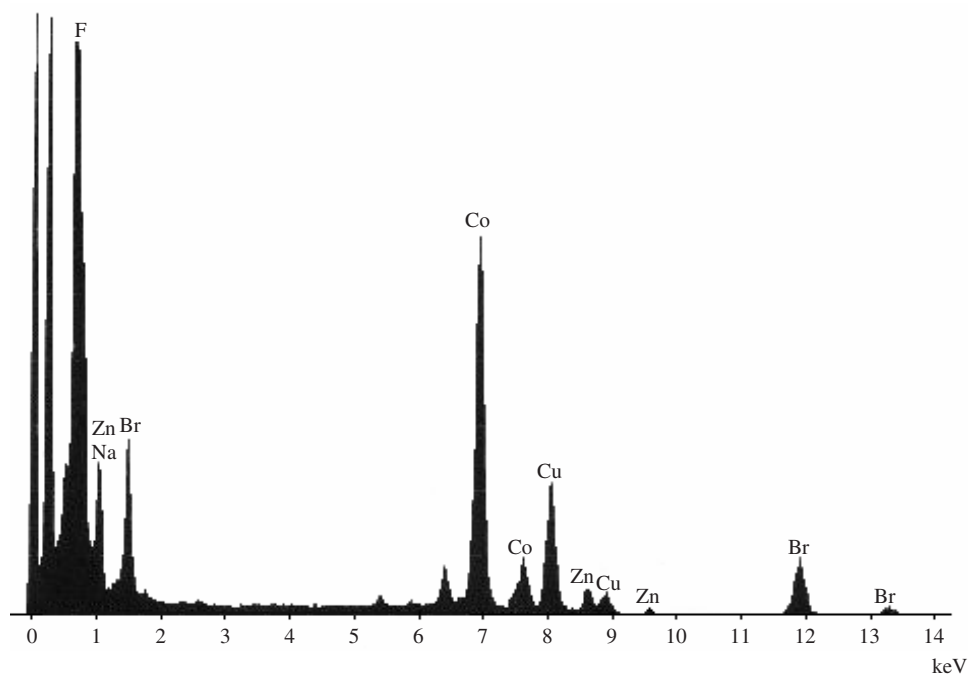

Figure 8. EDAX of the solid after reaction.

good dispersion. From the electron diffraction pattern of solid foam (figure 7b), two sets of interplanar space of crystallographic planes ($d = 2.96$ Å and 1.81 Å respectively) are obtained. According to the standard diffraction pattern of NaBr, these values match those of (200) and (311) planes very well. Therefore the crystallites appeared in the foam are confirmed to be NaBr crystallites.

It is accepted that such small but uniformly sized NaBr crystallites with excellent dispersion in F-Co(II) could not be obtained from direct crystallization (original NaBr in micron size) in $scCO_2$ as a solvent or modified solvent without the use of a micellar core as the template [44]. Zielinski *et al*. [45] characterized a micro-emulsion in $scCO_2$

which showed the micelle diameter to be in the range of 4.0–7.2 nm depending on the W_o ratio. Thus, the size and dispersion of NaBr crystals obtained are consistent with the micro-emulsion working state.

3.1.5 The effect of promoter.   As seen in figure 9, 0.02 mmol (in 111 mL autoclave) NaBr was shown to cause a significant attenuation in the initial activity compared with the original quantity (0.10 mmol). 0.05 mmol sodium bromide was shown to be just enough to achieve the maximum reaction rate at the beginning of the reaction. However, a slower rate was observed at higher conversions, which might have been caused by dilution of the NaBr with additional water produced from the reaction. Taking the whole volume of reactor into account, the concentration of NaBr used in the case of 0.05 mmol NaBr is approximately 4.4×10^{-4} M, which is much lower than those used in traditional liquid process using acetic acid as solvent (typical range of 10^{-2}–10^{-3} M [6]). However, considering the small amount of water as nano-droplets dispersed in scCO$_2$, the concentration of NaBr in the water could be pretty high (4.9×10^{-1} M) after deduction of the amount of water dissolved in scCO$_2$ (300 µL under the conditions in this study).

3.1.6 The effects of oxygen quantity.   It is generally known that mass transfer between gas and liquid phase is low such that it could become the rate-limiting step in conventional reactions involving gas-liquid interface. In order to enhance the reaction rate high pressures of dioxygen are usually used with vigorous stirring for the oxidation of alkyl aromatics in industry [46]. This could result in the associated difficulties in operations with potential explosion hazards. In the system being studied, it can be seen in figure 10 that the reaction rate was independent of the quantity of oxygen. 23.1 mmol O$_2$ (5.0 bar in 111 mL) gave a comparable reaction rate with excess O$_2$ of 46.2 mmol (O$_2$: toluene = 3 mol/mol). This suggests that a good miscibility of dioxygen in scCO$_2$ was established.
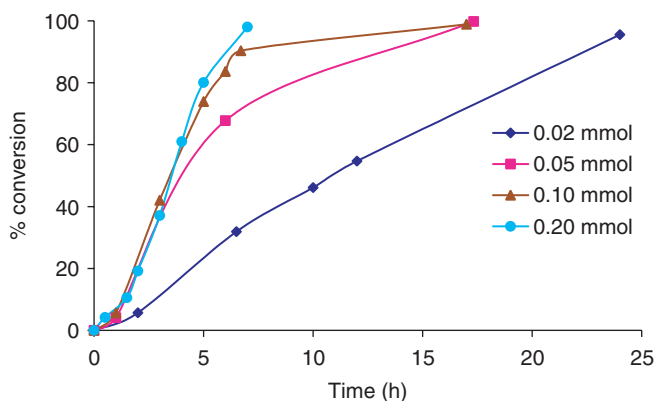

Figure 9.   Oxidation of toluene using various NaBr content (typical conditions: 0.25 mmol F-Co(II); various NaBr content as shown; 18.8 mmol toluene; 400 µL H$_2$O; 10 bar O$_2$ and 150 bar CO$_2$ at 120°C).

The explosion hazards associated with organic solvent and dioxygen at high concentration present one of the most difficult challenges in chemical industry. Reduction of dioxygen concentration in all cases is highly favorable. In this organic solvent free system, the high mass transfer of dioxygen to the micellar nano-reactor may provide a safer operation.

3.1.7 The effects of toluene concentration. To investigate the effect of toluene concentration on activity, experiments were carried out using various toluene concentrations (1.9×10^{-2} M, 4.8×10^{-2} M, and 7.6×10^{-2} M). From figure 11, it can be deduced that the shortest induction period is observed with highest concentration of toluene. Although the precise reason for this observation is not yet known, it is believed that the toluene concentration is related to the buildup of the concentrations of radicals (or other catalytic active species) to a critical level needed to ignite the reaction. After the reactions took off, the turnover frequencies, TOFs measured were 0.5×10^{-3} s^{-1} for
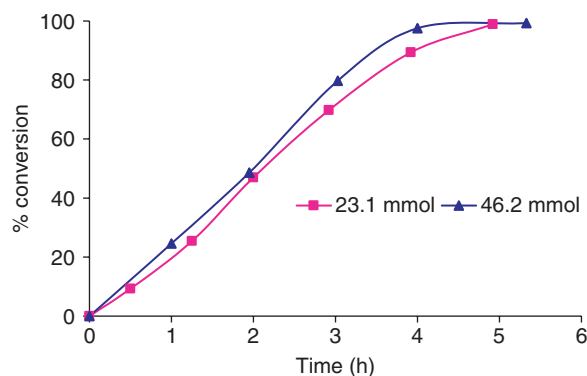

Figure 10. Effect of dioxygen quantity on percent of conversion (typical conditions: 0.25 mmol F-Co(II); 0.2 mmol NaBr; 15.8 mmol toluene; 400 µL H$_2$O; various O$_2$ pressure as shown and 150 bar CO$_2$ at 120°C).
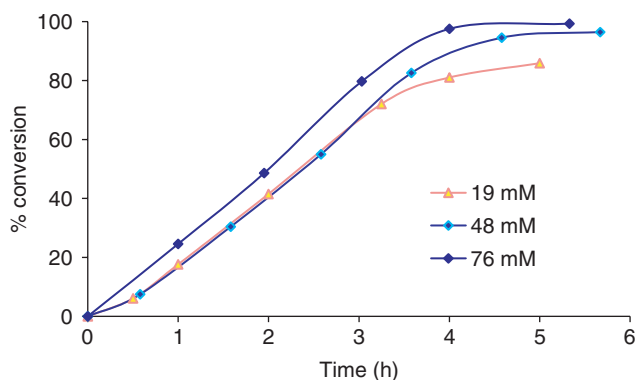

Figure 11. Effect of toluene concentration on activity (typical conditions: 0.25 mmol F-Co(II); 0.2 mmol NaBr; various toluene content as shown; 400 µL H$_2$O; 10 bar O$_2$ and 150 bar CO$_2$ at 120°C).
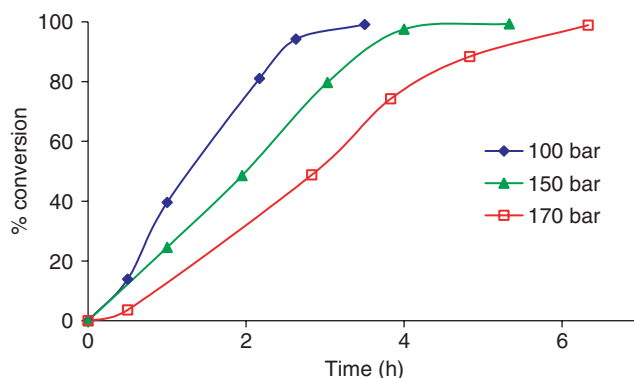
Figure 12.   Effect of pressure on activity (typical conditions: 0.25 mmol F-Co(II); 0.2 mmol NaBr; 14.1 mmol toluene; 400 μL H_2O; 10 bar O_2 and various applied $scCO_2$ pressures at 120°C).

19 mM, 1.4×10^{-3} s^{-1} for 48 mM, 1.98×10^{-3} s^{-1} for 76 mM of toluene respectively. It is interesting to note that these TOFs data were in a roughly first order function with respect to the toluene concentration. This linear relationship of the rate with respect to substrate concentration is consistent with those observed for most oxidation reactions of alkyl aromatics in solution [47], which suggests that the C–H activation (or C–H fission) in the toluene oxidation is likely be the rate limiting step.

3.1.8 The effect of scCO$_2$ pressure.   It can be seen from the figure 12 that the highest TOF was observed with the lowest total $scCO_2$ pressure amongst the three different pressures used (100 bar, 150 bar and 170 bar). The difference in activity could simply be related to the difference in toluene concentration in supercritical fluid: the highest toluene concentration was achieved with the lowest total carbon dioxide pressure for the same amount of toluene used in all the three cases. The selectivities of the reactions were also studied over the three cases. At high toluene conversions (99.1%, 99.3%, and 98.9% for 100 bar, 150 bar, and 170 bar, respectively), selectivities towards benzoic acid corresponded to 99.1%, 99.2%, 98.7% respectively. Thus, selectivities were nearly identical for the three cases within experimental error.

3.1.9 The effect of temperature.   Temperature is usually the critical factor for catalysis. Experiments under various temperatures (80°C, 100°C, 120°C) were carried out for the typical experimental conditions: 0.25 mmol F-Co(II); 0.2 mmol NaBr; 18.8 mmol toluene; 400 μL H_2O; 10 bar O_2 and 150 bar CO_2. It can be seen from figure 13 that the rate of the reaction strongly depends on the reaction temperature. A TOF of 6.48×10^{-3} s^{-1} and an induction period of 2.0 h were achieved at 120°C. A lower TOF of 2.86×10^{-3} s^{-1} and a longer induction period of 2.3 h were observed at 100°C. The activation energy of the system was estimated using equations (16) and (17) between 100–120°C to be 49.82 kJ/mol. The system was also studied at 80°C. However, only 8.5% of toluene was converted during the 24 hours. It is interesting to note that the rate of reaction did not fit with the estimated activation energy. Other factors
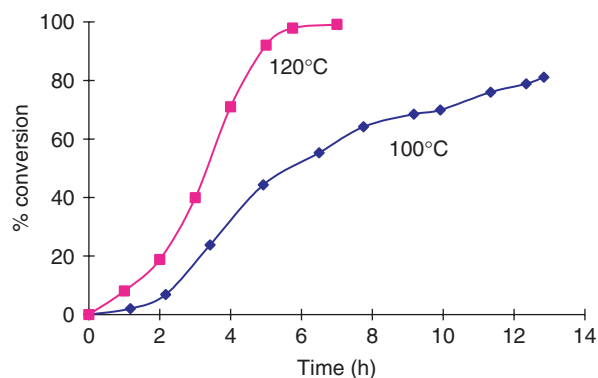
Figure 13. Effect of temperature on activity (typical conditions: 0.25 mmol F-Co(II); 0.2 mmol NaBr; 18.8 mmol toluene; 400 μL H_2O; 10 bar O_2 and 150 bar CO_2 at various temperature).

(i.e. morphology of micro-emulsion and its interfacial mass transfer) may contribute to this lower rate.

$$\ln\frac{k_1}{k_2} = \frac{E_a}{R}\left(\frac{1}{T_2} - \frac{1}{T_1}\right) \tag{16}$$

$$\frac{k_1}{k_2} = \frac{\{d[conversion]/dt\}_1}{\{d[conversion]/dt\}_2} = \frac{[Slope]_1}{[Slope]_2} \tag{17}$$

where: k_1 and k_2 are the rate constants for different temperature;
   Ea is the activation energy;
   R is the gas constant;
   T_1 and T_2 are reaction temperatures (in Kelvin);
   $(Slope)_1$ and $(Slope)_2$ are the slopes calculated from figure 13 at T_1 and T_2 respectively.

3.1.10 Kinetic isotope effect. In order to provide further insight into the mechanism of the reaction, kinetic isotope effect (KIE) on reaction rate was investigated by replacing normal toluene with deuterated d_8-toluene (99 atom D%, Aldrich) during catalysis. The isotope effect mainly originates from the difference of zero point energy (a minimum amount of vibrational frequency due to the Heisenberg uncertainty principle) between RH (R-alkyl) and RD (equation (18)) thus using d-toluene instead of normal toluene could slow down the reaction if the activation of hydrocarbon is involved in the rate limiting step.

$$\ln\left(\frac{k_H}{k_D}\right) = \ln\left(\frac{A_H}{A_D}\right) - \left(\frac{\Delta E}{RT}\right) \tag{18}$$
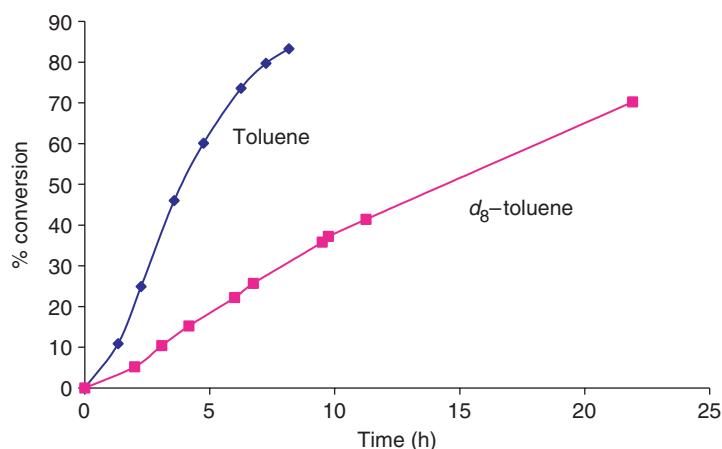
Figure 14. Kinetic isotope effect observed by replacing normal toluene with deuterated toluene (typical conditions: 0.20 F-Co(II); 0.2 mmol NaBr; 14.1 mmol toluene or d_8-toluene; 400 μL H_2O; 10 bar O_2 and 150 bar CO_2 at 120°C).

where,

k_H and k_D are the rate constant of R-D and R-H respectively during oxidation;
A_H and A_D are the pre-exponential factor of R-D and R-H respectively;
ΔE is the difference of zero point energy between R-H and R-D.

The k_H/k_D was estimated to be 3.4 from figure 14. This clearly suggests that the fission of C–H bond of toluene is the rate-determining step, which is also consistent with the effect of toluene concentration. A k_H/k_D value was shown as 2.25 in the literature for the liquid phase Mid-century process [2], which is lower than the present system. This suggests that the present mechanism may not be identical to that of the traditional process, which implies catalysis using nano-droplets may significantly differ to that in bulk solution.

3.1.11 The reusability of catalyst.　One of the greatest concerns in catalysis studies is the reusability and deactivation of this nanocatalyst system in supercritical carbon dioxide. As a result, a brief study on the reusability of the catalyst system was carried out (figure 15).

The first run was carried out using fresh catalyst under the typical conditions. At the end of experiment, the reaction mixture was quenched by a rapid depressurisation of the CO_2 to the ambient pressure once it was cooled. The second run was then carried out by adding the same quantity of toluene to the autoclave reactor. The results presented in figure 15 represent the 1st and 2nd subsequent tests. The preliminary results clearly show that the high conversions were achieved within the 12 hour run time in both the cases. This suggests that the micellar catalyst system can be reconstructed in scCO₂ during the subsequent testing. Detailed comparison of the rates of reaction at different times between 1st and 2nd subsequent test indicated no sign of deactivation. A shorter induction period and higher reaction rate were actually observed in the second run. This may be attributed to the existence of Co^{3+} and benzylaldehyde (catalytic active species
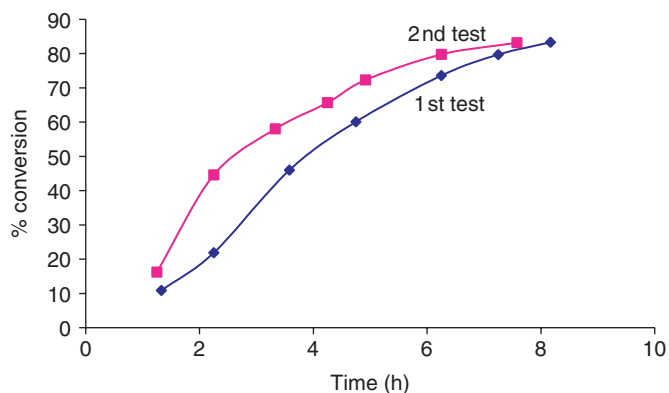
Figure 15. Reusability of nano-catalyst system (typical conditions: 0.2 mmol F-Co(II); 0.2 mmol NaBr; 4.7 mmol toluene; 400 μL H_2O; 10 bar O_2 and 150 bar CO_2 at 120°C).

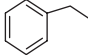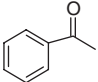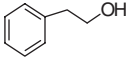generated in the 1st run) at the beginning of the 2nd run. Both of these could speed up the oxidation reaction.
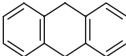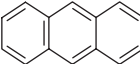
3.1.12 Oxidation of bulk alkyl aromatic hydrocarbons. The results on the oxidation of other alkyl aromatics using F-Co(II) in the presence of NaBr and water are presented in table 3.

Table 3 clearly shows that F-Co(II) in nano-water droplets in $scCO_2$ catalyses oxidations of other alkylaromatic molecules with considerable high conversions and selectivities towards selective products. The oxidations of ethyl-benzene, dihydro-anthracene and 2-methyl an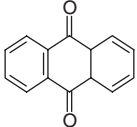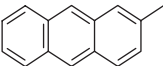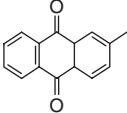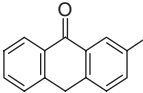thracene gave acetophenone (83.7%), anthracene (67.6%) and 2-methyl-anthraquinone (76.3%) as the main products, respectively. It is thus apparent from the table that the novel catalyst system is equally effective for the oxidation of other bulky alkyl aromatic hydrocarbons in supercritical carbon dioxide. These non-polar bulky hydrocarbons generally display a low solubility in acetic acid, and are rather non-volatile at elevated temperatures (with correspondingly poor activity in gas phase reactions). In contrast, they are expected to give a considerable solubility in $scCO_2$ phase [48]. Thus, water-$scCO_2$ nano-catalyst system is envisaged to provide an ideal medium for their catalysis.

4. Conclusions

The water-$scCO_2$ micro-emulsion system is shown to be an excellent alternative solvent to acetic acid for the important Co(II) oxidation of alkyl aromatics processes. The organic-free ligand/stabilizer and solvent system containing no C–H structure with an excellent dispersion of Co(II)/NaBr species are well suited for ultraselective oxidation reactions. In addition, the generic concept of using the H_2O-$scCO_2$ micro-emulsion to bring species of a very different polarity into contact with excellent mass and heat transfers in sustaining a fast catalytic reaction could be utilized for a wide range of oxidations. H_2O-$scCO_2$ as a solvent will exhibit real advantages by providing a 'green'

Table 3. Oxidations of other alkyl aromatic hydrocarbons.

Substrate	Catalysts	Conv. (%)	Select (%)	
	F-Co(II)/NaBr	49.2	83.7	
			16.3	
	F-Co(II)/NaBr	99.2	67.6	
			32.4	
	F-Co(II)/NaBr	64.2	76.3	
			23.7	

Typical conditions: 0.25 mmol F-Co(II); 0.2 mmol NaBr; 100 μL H_2O; 10 bar O_2 and 150 bar CO_2 at 120$°$C.

process with safer operation, easier separation and purification, high catalytic activity with selectivity and with no loss of solvent by oxidation. It is believed that the novelty of dispersing hydrophilic and/or ionic species into hydrophobic supercritical phase using water-scCO_2 micro-emulsion is of great importance in catalysis because a wide range of water-soluble catalysts can be employed in micelles as nano-reactors to carry out catalytic oxidations in scCO_2.

References

[1] A.K. Suresh, M.M. Sharma, T. Sridhar. Engineering aspects of industrial liquid-phase air oxidation of hydrocarbons. *Ind. Eng. Chem. Res.*, **39**, 3958 (2000).
[2] L.A. Burrows, R.M. Cananaugh. US Pat. 2636899 (1953).

[3] P. Boffa, R. Costeballa, G. Maiorano. Fr. Pat. 1299913 (1962).

[4] C.A. Spiller. US Pat. 2962361 (1960).

[5] A. Saffer, R.S. Barker. US Pat. 2833816 (1958).

[6] W. Partenheimer. Methodology and scope of metal bromide autoxidation of hydrocarbons. *Catal. Today*, **23**, 69 (1995).

[7] Y. Kamiya, M. Kashima. Autooxidation of aromatic hydrocarbons catalyzed with cobaltic acetate in acetic acid solution. 1. Oxidation of toluene. *J. Catal.*, **25**, 326 (1972).

[8] K. van der Wiele, P.J. van den Berg. Oxidation of toluene over bismuth molybdate catalysts. *J. Catal.*, **39**, 437 (1975).

[9] R.A. Sheldon, J.K. Kochi. *Metal-catalyzed Oxidations of Organic Compounds*, Chapter 7, Academic Press, New York (1981).

[10] K. Weissermel, H.-J. Arpe. *Industrial Organic Chemistry*, C.R. Lindley, translator, 2nd ed., VCH:, Weinheim, Germany (1993).

[11] S.W. Benson, P.S. Nangia. Some unresolved problems in oxidation and combustion. *Acc. Chem. Res.*, **12**, 223 (1979).

[12] N.M. Emanuel, E.T. Denisov, Z.K. Maizus. *Liquid-phase Oxidation of Hydrocarbons*, Plenum Press, New York (2000) p. 71.

[13] K. Nakaoka, Y. Miyama, S. Matsuhisa, S. Wakamatsu. Preparation of terephthalic acid using paraldehyde promoter. *Ind. Eng. Chem. Prod. Res. Develop.*, **12**, 150 (1973).

[14] W.F. Brill. Terephthalic Acid by Single-Stage Oxidation. *Ind. Eng. Chem.*, **52**, 837 (1960).

[15] K. Sawada, M. Tanaka. Formation of bromo complexes of cobalt(II) in acetic acid. *J. Inorg. Nucl. Chem.*, **39**, 339 (1977).

[16] W.D. Bardsley, R.L. Falles, R. Hunter, V.R. Stimson. Catalysis of radical chain reactions. *J. Chem. Ed.*, **61**, 657 (1984).

[17] E. Sahle-Demessie, M.A. Gonzalez, J. Enriquez, Q. Zhao. Selective oxidation in supercritical carbon dioxide using clean oxidants. *Ind. Eng. Chem. Res.*, **39**, 4858 (2000).

[18] S.A. Chavan, S.B. Halligudi, D. Srinivas, P. Ratnasmy. Formation and role of cobalt and manganese cluster complexes in the oxidation of p-xylene. *J. Mol. Catal. A*, **161**, 49 (2000).

[19] V. Parvulescu, C. Anastasescu, C. Constantin. Mono (V, Nb) or bimetallic (V-Ti, Nb-Ti) ions modified MCM-41 catalysts: synthesis, characterization and catalysis in oxidation of hydrocarbons (aromatics and alcohols). *Catal. Today*, **78**, 477 (2003).

[20] C. Subrahmanyam, B. Louis, F. Rainone, B. Viswanathan, A. Renken, T.K. Varadarajan. Catalytic oxidation of toluene with molecular oxygen over Cr-substituted mesoporous materials. *Appl. Catal. A*, **241**, 205 (2003).

[21] T.W. Bastock, J.H. Clark, K. Martin, B.W. Trenbirth. Mild, solvent-free oxidation of toluene and substituted toluenes to their benzoic acids using carboxylic acid-promoted heterogeneous catalysis. *Green Chem.*, **4**, 615 (2002).

[22] A.I. Anastasov. Deactivation of an industrial V_2O_5-TiO_2 catalyst for oxidation of o-xylene into phthalic anhydride. *Chem. Eng. Process*, **42**, 449 (2003).

[23] B.K. Das, J.H. Clark. A novel immobilised cobalt(III) oxidation catalyst. *Chem. Commun.*, **7**, 605 (2000).

[24] W.X. Kuang, Y.N. Fan, K.D. Chen, Y. Chen. Partial oxidation of toluene over ultrafine mixed Mo-based oxide particles. *J. Catal.*, **186**, 310 (1999).

[25] J. Miki, Y. Osada, T. Konoshi, Y. Tachibana, T. Shikada. Selective oxidation of toluene to benzoic acid catalyzed by modified vanadium oxides. *Appl. Catal. A*, **137**, 93 (1996).

[26] Y. Liu, Y. Lu, P. Liu, R. Gao, Y. Yin. Effects of microwaves on selective oxidation of toluene to benzoic acid over a V_2O_5/TiO_2 system. *Appl. Catal. A*, **170**, 207 (1998).

[27] D.A. Bulushev, L. Kiwi-Minsker, A. Renken. Transient kinetics of toluene partial oxidation over V/Ti oxide catalysts. *Cata. Today*, **61**, 271 (2000).

[28] J.M. Desimone, E.E. Maury, Y.Z. Meneceloglu, J.B. Mcclain, T.J. Romack, J.R. Combes. Dispersion polymerizations in supercritical carbon dioxide. *Science*, **265**, 356 (1994).

[29] R.J. Klingler, J.W. Rathke. High-pressure NMR investigation of hydrogen atom transfer and related dynamic processes in oxo catalysis. *J. Am. Chem. Soc.*, **116**, 4772 (1994).

[30] M.G. Hitzler, M. Poliakoff. Continuous hydrogenation of organic compounds in supercritical fluids. *Chem. Commun.*, **17**, 1667 (1997).

[31] J. Zhu, A. Robertson, S.C. Tsang. Aqueous emulsion containing fluorous cobalt species in supercritical CO_2 for catalytic oxidation of toluene. *Chem. Commun.*, **18**, 2044 (2002).

[32] K.P. Johnston, K.L. Harrison, M.J. Clarke, S.M. Howdle, M.P. Heitz, F.V. Bright, C. Carlier, T.W. Randolph. Water in carbon dioxide microemulsions: an environment for hydrophiles including proteins. *Science*, **271**, 624 (1996).

[33] D.E. Fremgen, E.S. Eugene, R.E. Gerald, R.J. Klingler, J.W. Rathke. Microemulsions of water in supercritical carbon dioxide: an in-situ NMR investigation of micelle formation and structure. *J. Supercrit. Fluids*, **19**, 287 (2001).

[34] P.A. Psathas, E.A. Sander, M.Y. Lee, K.T. Lim, K.P. Johnston. Mapping the stability and curvature of emulsions of H_2O and supercritical CO_2 with interfacial tension measurements. *J. Disper. Sci. Tech.*, **23**, 65 (2002).

[35] R.E. Banks. *Fluorocarbons and their Derivatives*, Spottiswoode, Ballantyne & Co. Ltd., London (1964) p. 16.

[36] B. Schrader (Ed.). *Raman/Infrared Atlas of Organic Compounds*, 2nd ed., B3–29, Weinheim: VCH (1989).

[37] K.D. Bartle, A.A. Clifford, S.A. Jafar, G.F. Shilstone. Solubilities of solids and liqids of low volatility in supercritical carbon dioxide. *J. Phys. Chem.*, **20**, 728 (1991).

[38] A.V. Yazdi, E.J. Beckman. Design, synthesis, and evaluation of novel, highly CO_2-soluble chelating agents for removal of metals. *Ind. Eng. Chem. Res.*, **35**, 3644 (1996).

[39] Y.H. Lin, R.D. Brauer, K.E. Laintz, C.M. Wai. Supercritical fluid extraction of lanthanides and actinides from solid materials with a fluorinated beta-diketone. *Anal. Chem.*, **65**, 2549 (1993).

[40] J. Eastoe, B.M.H. Cazelles, D.C. Steytler, J.D. Holmes, A.R. Pitt, T.J. Wear, R.K. Heenan. Water-in-CO2 microemulsions studied by small-angle neutron scattering. *Langmuir*, **13**, 6980 (1997).

[41] R. Wiebe. The binary system carbon dioxide-water under pressure. *Chem. Rev.*, **29**, 475 (1941).

[42] M.P. Czytko, G.K. Bub. Oxidation of toluene by cobalt(III) acetate in acetic acid solution. Influence of water. *Ind. Eng. Chem. Prod. Rev. Dev.*, **20**, 481 (1981).

[43] K.M. Dooley, F.C. Knopf. Oxidation catalysis in a supercritical fluid medium. *Ind. Eng. Chem. Res.*, **26**, 1910 (1987).

[44] M. Ji, X. Chen, C.M. Wai, J.L. Fulton. Synthesizing and dispersing silver nanoparticles in a water-in-supercritical carbon dioxide microemulsion. *J. Am. Chem. Soc.*, **121**, 2631 (1999).

[45] R.G. Zielinski, S.R. Kline, E.W. Kaler, N. Rosov. A small-angle neutron scattering study of water in carbon dioxide microemulsions. *Langmuir*, **13**, 3934 (1997).

[46] K. Nakaoka, Y. Miyama, S. Matsuhisa, S. Wakamatsu. Preparation of Terephthalic acid using paraldehyde promoter. *Ind. Eng. Chem. Prod. Res. Dev.*, **12**, 150 (1973).

[47] Y. Kamiya. Catalysis by cobalt and bromide ions in autoxidation of alkylbenzenes in acetic acid. *J. Catal.*, **33**, 480 (1974).

[48] A. Baiker. Supercritical fluids in heterogeneous catalysis. *Chem. Rev.*, **99**, 453 (1999).